Ecohydrology

WILEY

RESEARCH ARTICLE OPEN ACCESS

Continuous Stem Water Potential Measurements of a Diffuse-Porous Tree Species Offer New Insights Into Tree Water Relations

Simon Haberstroh[1] | Fabio Scarpa[1] | Stefan Seeger[2] | Andreas Christen[3] | Christiane Werner[1]

[1]Ecosystem Physiology, Faculty of Environment and Natural Resources, University Freiburg, Freiburg, Germany | [2]Soil Physics, Department of Crop Sciences, University of Göttingen, Göttingen, Germany | [3]Environmental Meteorology, Faculty of Environment and Natural Resources, University Freiburg, Freiburg, Germany

Correspondence: Simon Haberstroh (simon.haberstroh@cep.uni-freiburg.de)

Received: 25 July 2024 | **Revised:** 9 December 2024 | **Accepted:** 1 January 2025

Funding: This study was funded by SFB1537 (ECOSENSE, Deutsche Forschungsgemeinschaft).

Keywords: *Carpinus betulus* | midday water potential | predawn water potential | sap flow

ABSTRACT

Water potential is a crucial parameter for assessing tree water status and hydraulic strategies. However, methods for measuring water potential, such as the Scholander pressure chamber, are destructive, discontinuous and difficult to perform in tall forests. Consequently, important dynamics in water potentials, particularly during short-term drought, are difficult to capture. Recent advancements have introduced low-maintenance sensors capable of measuring continuous, high-resolution stem water potentials.

We evaluated these sensors in a temperate, diffuse-porous species (*Carpinus betulus*) over a growing season marked by dry-down periods and heat. Measurements of leaf water potential, sap flow and environmental factors (air temperature, vapour pressure deficit and soil water content) were conducted. Midday stem water potentials of *C. betulus* reached minimum values of -3.39 ± 0.10 MPa and exhibited pronounced seasonal fluctuations, mirroring changes in environmental conditions and sap flow. Stem water potentials correlated well with Scholander-type measurements during predawn ($R^2 = 0.98$) but demonstrated an offset in absolute values during midday ($R^2 = 0.71$) and diurnal measurements. Minimum stem water potentials and maximum sap flow in the stem expressed a time lag and showed a distinct hysteresis. In this first assessment, the agreement with Scholander-type measurements, sap flow and environmental parameters suggests the tested water potential sensors yield reliable data, especially during predawn, but need further validation during midday conditions. If applicable to other tree species, these sensors could significantly advance our understanding of tree water relations and their role in forest drought responses.

1 | Introduction

Water potential gradients in the soil–plant-atmosphere continuum are the main driving force for water movements in plants, such as transpiration or sap flux in the xylem (e.g., Philip 1966; Larcher 1994). These gradients can be strongly modified by plant external (e.g., edaphic or atmospheric aridity) or plant internal factors (e.g., xylem architecture, stomatal control and stem capacitance) (Choat et al. 2018), which lead to diurnal and seasonal water potential variations within plants. These water potential variations can be used as an integrative and valuable parameter for assessing plant water status, plant hydraulic strategies or plant drought resistance and resilience (Larcher 1994; Steppe 2018; Torres-Ruiz et al. 2024). Declining water potentials in plants, e.g., under edaphic drought, can have cascading effects on several vital processes. In general, leaf stomatal

conductance is reduced as a first response to declining water potentials, which strongly reduces plant water fluxes, and thereby also photosynthetic carbon assimilation and thus, plant growth and production (Brodribb 2009; McDowell 2011; Torres-Ruiz et al. 2024). Under severe drought, plant water potentials can drop below species-specific thresholds, triggering xylem cavitation and threatening plant survival (Choat et al. 2018; Schuldt et al. 2020; Mantova et al. 2022).

These examples demonstrate that water potential gradients and water potentials in plants are related to a plethora of important and vital plant processes. However, measurements of plant water potential are mostly still limited to single points in time and space, which restricts our knowledge on important biophysical responses to plant stress (reviewed in Novick et al. 2022). For example, a combination of sap flow and continuous water potential measurements could help, amongst others, to elucidate the dynamic control of water potential on plant water fluxes under edaphic or atmospheric drought, but also vice versa the buffering of plant water potentials by other processes, e.g., by capacitive discharge of stored water into the transpiration stream in times of water scarcity (Scholz et al. 2011; McCulloh et al. 2019; Martín-Gómez et al. 2023). To confront the so-called 'water potential information gap' (Novick et al. 2022), continuous, high-resolution water potential measurements are urgently needed to advance our knowledge in the field of plant water relations.

Up to date, the majority of plant water potentials are still measured using the Scholander pressure chamber (Scholander et al. 1965). While this method is well established and provides a robust way of assessing plant water potentials, measurements are time- and labour-consuming (Steppe 2018), destructive, sensitive to user errors (Rodriguez-Dominguez et al. 2022) and most importantly, do not provide the needed continuous data (Novick et al. 2022). For example, Guo et al. (2020) demonstrated a highly dynamic hydraulic behaviour in the shrub *Larrea tridentata* with continuous water potential measurements, spanning from extreme anisohydric to partial isohydric in the course of only one growing season. Similarly, *Quercus suber* trees shifted their hydraulic behaviour not only from wet to dry seasons but also in response to species competition (Haberstroh et al. 2022a). While high-frequency measurements (or the installation of expensive, high-maintenance sensors, such as stem psychrometers) are in general viable for smaller vegetation (e.g., Guo et al. 2020), frequent measurements on tall forest trees are more challenging (Steppe 2018), as either canopy access towers (e.g., Haberstroh et al. 2022b) or professional tree climbers are required to reach the tree crown for accurate measurements (e.g., Kinzinger et al. 2024).

In recent years, new methods to indirectly obtain continuous water potentials have been developed and successfully applied, such as the use of point (Dietrich, Zweifel, and Kahmen 2018; Ziegler et al. 2024), optical (Bourbia et al. 2023) or contact dendrometers (Gleason et al. 2024). While promising and inexpensive, dendrometers need to be regularly calibrated against Scholander pressure chamber measurements over a large range of water potentials, as the relationship of stem diameter changes and water potentials is rather non-linear (Dietrich, Zweifel, and Kahmen 2018; Gleason et al. 2024; Ziegler et al. 2024) and might be species and site-specific. As a viable alternative, sensors based on microtensiometers were developed, which offer direct measurements of water potentials in the stem or trunk. Measurements in important agricultural and horticultural woody species, such as apple (e.g., González et al. 2022; Blanco and Kalcsits 2024), pear (Blanco and Kalcsits 2023), olive (Villalobos et al. 2024), grapevine or almond (Lasko, Santiago, and Stroock 2022), indicate a general agreement with traditional Scholander-type pressure chamber measurements, although Blanco and Kalcsits (2023) demonstrated some inaccuracies of microtensiometers in the stem to correctly capture water potentials in the afternoon.

Our main objective was to evaluate sensors for continuous stem water potential measurements and determine their general accuracy, applicability and limitations for ecophysiological research in forest trees. To demonstrate potential applications of continuous water potential data, we aim to dynamically investigate how plant water fluxes and water potentials are coupled in plants under varying environmental conditions, such as atmospheric and edaphic drought. To evaluate the sensors, we chose the deciduous broadleaf hornbeam (*C. betulus* L.) without notable resin production. A diffuse-porous species was chosen from previous experience with the unproblematic installation of in situ probes in the tree xylem (i.e., for water stable isotope measurements, Kinzinger et al. 2024).

2 | Material and Methods

2.1 | Field Site and Tree Species

(*C. betulus*) trees at the Hartheim (Germany, 7.59814° E, 47.93391° N, 201 m a.s.l.) forest research site, an ICOS ecosystem site (DE-Har) operated by the University of Freiburg (Haberstroh et al. 2022b). The site is located on the alluvial plain of the Upper Rhine with an average groundwater table at 7 m below the surface. For the period of 1991–2020, the field site's climate was characterized by an average air temperature of 10.6°C and average annual precipitation of 646 mm. The forest research site was formerly dominated by *Pinus sylvestris*; however, recent drought and heat events in combination with unfavourable site conditions (low groundwater table, shallow and sandy soils) initiated a vegetation shift towards broadleaved understory trees. One of the dominant understory species is *C. betulus* (21% of all understory trees), which was more resistant during past drought events compared to *P. sylvestris* (Haberstroh et al. 2022b). The three chosen trees had a height of 10.0–10.5 m, a diameter at breast height of 16.0–18.7 cm and were growing in close vicinity to a 30 m canopy access tower to allow accessibility of tree crowns for leaf water potential measurements.

2.2 | Meteorological Measurements

Air temperature (T_{air}), relative humidity and vapour pressure deficit (VPD) were measured on site 2 m above ground in the forest canopy with an actively ventilated psychrometer. Precipitation was measured above the canopy (18 m) with an Ombrometer Model 5.4031 (Adolf Thies, Germany). Volumetric soil water content (VWC) was measured in two profiles and

three depths (0.05, 0.10, 0.20, 0.50 and 1.00 m using CS655 soil moisture and temperature sensors, Campbell Scientific Logan, UT, USA). VWC values were averaged over the first three depths (0.05–0.20 m) and both profiles to describe a general trend of VWC in the topsoil.

2.3 | Installation and Operation of Stem Water Potential Sensors

Stem water potential sensors (microtensiometers, piezoresistive pressure transducer, FloraPulse, CA, USA) with a size of 5 × 5 mm held in a cylindrical probe (8 mm diameter) were installed in May 2023 (cf. Lasko, Santiago, and Stroock 2022; Pagay 2022). In detail, we installed the provided sleeve (14 mm outer diameter, 9 mm inner diameter) in the stem and ensured the xylem tissue was reached. Stem material within the sleeve was drilled to a depth of ~4–5 cm and removed carefully. All installation points showed a bright white colour, which was identified as active xylem tissue. Afterwards, the sleeve was immediately filled with the mating compound (fine clay paste, Lasko, Santiago, and Stroock 2022) provided by FloraPulse before the sensor (8 mm cylindrical probe) was carefully inserted and tightened with a spring and cap. To avoid water infiltration, the sleeve and sleeve hole were covered with silicone grease (Figure S1). Installation occurred ~1 m above the ground and sensors were shielded with reflective aluminium foil to avoid thermal influences of radiation. No further maintenance was required until November 2023, when sensors were deinstalled. Stem water potential (Ψ_{Stem}) data was collected every 20 min on a Campbell CR1000 logger (Campbell Scientific, UT, USA). Predawn water potential (Ψ_{PD}) was calculated by averaging the measured values 2 h before sunrise. Midday water potential (Ψ_{MD}) was calculated by averaging values 2 h after solar noon (CEST).

2.4 | Scholander Pressure Chamber Measurements

Scholander-type pressure chamber (1505D, PMS Instrument, USA) measurements (Scholander et al. 1965) were conducted predawn and midday over the course of the growing season from May to September 2023 at 6 days on terminal branchlets of *C. betulus*, which represented leaf water potentials (Ψ_{Leaf}). Predawn water potential was measured between 4 and 6 AM (CEST), but always before sunrise. Midday measurements were conducted between 1 and 3 PM (CEST) on sunlit, uncovered, branchlets of *C. betulus*, approximately 8–10 m aboveground on sunny days. It should be noted that Ψ_{Leaf} is therefore always expected to be more negative than Ψ_{Stem} during daytime, given both their exposure to the sun and the difference in canopy height. On 7 September, Scholander-type measurements were conducted every 1–2 h from 6 AM to 10 PM (CEST).

2.5 | Sap Flow Measurements

In May, sap flow sensors (SFM1, ICT International, Armidale, Australia) were installed on the selected *C. betulus* trees at ~1.20 m height in close proximity to stem water potential sensors. Sensors consisted of three 35 mm stainless-steel needles that were installed in the xylem to measure sap flow at 12.5 and 27.5 mm depths from the cambium. The needle placed in the middle served as a heating element. Heat pulses (30 J) were generated every 20 min and data stored on internal loggers. Sap flux density (J_s) was calculated with the Heat Ratio Method (HRM, Marshall 1958; Burgess et al. 2001) and averaged for both measured xylem depths. In nights with zero sap flow between May and November (defined as photosynthetically active photon flux density $< 5\,\mu mol\,m^{-2}\,s^{-1}$, VPD < 0.05 kPa, $T_{air} > 0°C$, RH > 95%), we corrected J_s for offsets from the baseline (defined as zero sap flow).

2.6 | Statistical Analysis

For the comparison of Ψ_{Stem} and Ψ_{Leaf}, we calculated a regression (linear mixed-effect model) using the function *lme* in the R package *nlme* (Pinheiro et al. 2023) with tree identity as random effect (random intercept) (Equation **S1**). For the relationship of Ψ_{MD} calculated from Ψ_{Stem}, we applied linear mixed-effect models with T_{air} and maximum daily VPD (VPD_{max}) as predictors, respectively (Equations S3 and S4). Midday data were square root transformed to comply with model assumptions. No clear relationship of Ψ_{PD}, calculated from Ψ_{Stem} and T_{air} or VPD_{max}, was found. The relationship between Ψ_{Stem} (predawn and midday) and VWC was best described by asymptotic regressions with the function *nlme* (Pinheiro et al. 2023) (Equation S5).

To compare diurnal values of Ψ_{Stem} and Ψ_{Leaf}, we calculated linear regressions (*lm*) for each tree separately (Equation S2). Depending on the tree individual, there was a lag between daily minimum Ψ_{Stem} and Ψ_{Leaf}. This lag was determined by the best fit between both parameters, i.e., by increasing the lag in 20-min steps until the best R^2 of the regression was found.

The relationship of daily J_s sum and mean daily VPD (VPD_{mean}) was assessed with a non-linear mixed-effect models in the form of $J_s = aVPD_{mean} + bVPD_{mean}^2$ (Equation S7) using the function *lme* in the R package *nlme* (Pinheiro et al. 2023). Here, VPD_{mean} was a stronger predictor of J_s than VPD_{max}. The relationship was assessed for two different periods based on a threshold of 13% (VWC), which was determined by a visual assessment of data in combination with literature values (cf. Sánchez-Costa, Poyatos, and Sabaté 2015; Haberstroh et al. 2022a). In all of these mixed effect models, tree identity was treated as random effect (random intercept). The relationship of daily J_s sum and mean daily Ψ_{Stem} indicated an upper limit of J_s at a given Ψ_{Stem}. Thus, we determined the maximum J_s for Ψ_{Stem} intervals of 0.1 MPa (large points in Figure 7) to fit a linear regression (*lm*) of maximum J_s and Ψ_{Stem} (similar to Brandes et al. (2007) for canopy conductance and VPD) (Equation S6). Data were only used when VWC was below the threshold of 13%. In both models, only daytime values between sunrise and sunset were used.

Model assumptions of linear mixed-effect models (normal distribution of residuals) were tested with the Shapiro–Wilk test (*shapiro.test* in package *stats*, R Core Team 2022). Conditional (R^2_c) and marginal R^2 (R^2_m) were obtained using the function *r.squared.GLMM* available in the R package *MuMIn* (Bartoń 2022) for linear mixed-effect models (*lme*) and with the

function *R2M* in the package *nlraa* (Miguez 2023) for non-linear mixed-effect models (*nlme*). Details on all statistical models, model parameters and summaries can be found in Material and Methods S1, Equations S1–S7, Table S1-S12. All statistical analysis was conducted with the open-source software R (version 4.2.1, R Core Team 2022).

3 | Results

3.1 | Meteorological Conditions

2023 was characterized by a wet and moderately warm spring (Mar–May, +0.55 K warmer than 1991–2020). This was followed by a summer (Jun–Aug) with much higher T_{air} (+1.53 K) and declining VWC from May onwards (Figure 1). Two distinct periods with high T_{air} were identified on 9 July (T_{max}: 36.1°C) and on 19 August 2023 (T_{max}: 36.2°C), where daily maximum VPD (VPD_{max}) increased to values >4 kPa (Figure 1A). A steep decline of VWC from ~27% to <10% occurred from mid-May to mid-June, where almost no precipitation was recorded (Figure 1B). Despite frequent summer precipitation in July, VWC did not recover until November 2023. An analysis of meteorological conditions for the whole year showed that 2023 was the warmest year (12.3°C, +1.7 K) at the field site since climate records in 1978, while precipitation (606 mm, −40 mm) was close to the long-term average.

3.2 | Seasonal Development of Stem Water Potential and Sap Flux Density

Environmental conditions (Figure 1) were reflected in water potentials and sap flux density (J_s) of *C. betulus* (Figure 2). From May to July, Ψ_{Stem} decreased from values close to 0 MPa to −1.03 ± 0.16 MPa (Ψ_{PD}, Figure 2A) and −2.37 ± 0.21 MPa (Ψ_{MD}, Figure 2B). Afterwards, Ψ_{Stem} developed more dynamically due to more frequent precipitation events (Figure 1B) until a distinct dry-down period with high T_{air} was observed in mid-August, leading to minimum Ψ_{PD} (−1.59 ± 0.13 MPa) and Ψ_{MD} (−3.39 ± 0.10 MPa). For predawn conditions, continuous Ψ_{Stem} and destructive Ψ_{Leaf} measurements showed a good agreement in dynamics and absolute values with the expectation of late August 2023, where Ψ_{Leaf} dropped to −2.27 ± 0.19 MPa compared to −1.49 ± 0.14 MPa of Ψ_{Stem} (Figure 2A). Under midday conditions, Ψ_{Leaf} also resembled the dynamics of Ψ_{Stem}; however, absolute values were mostly lower, particularly visible in September 2023 (with one exception in mid-August 2023, where Ψ_{Stem} was lower compared to Ψ_{Leaf}, Figure 2B). Both, Ψ_{PD} and Ψ_{MD}, extracted from Ψ_{Stem} recovered to values close to 0 MPa during the rewetting period in early October.

J_s of *C. betulus* increased in spring 2023 in accordance with rising T_{air} and VPD_{max} (Figure 1A) to maximum values of 235.7 ± 25.0 $cm^3\,cm^{-2}\,day^{-1}$. With declining VWC, J_s decreased over the first half of summer, similarly to Ψ_{Stem}, until July. Afterwards, dynamics in J_s mostly resembled dynamics in

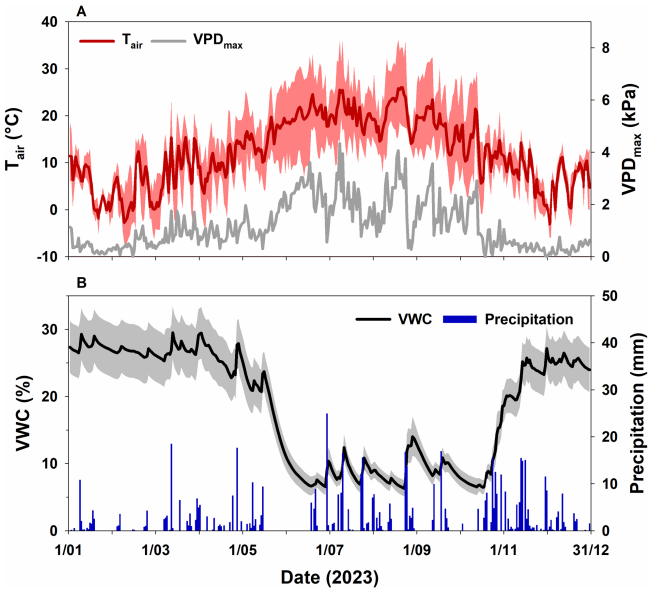

FIGURE 1 | Seasonal development of daily average air temperature (T_{air}) with maximum and minimum T_{air}, maximum vapour pressure deficit (VPD_{max}) (both A), volumetric soil water content (±1 SE) and precipitation (both B) at the forest research site in Hartheim.

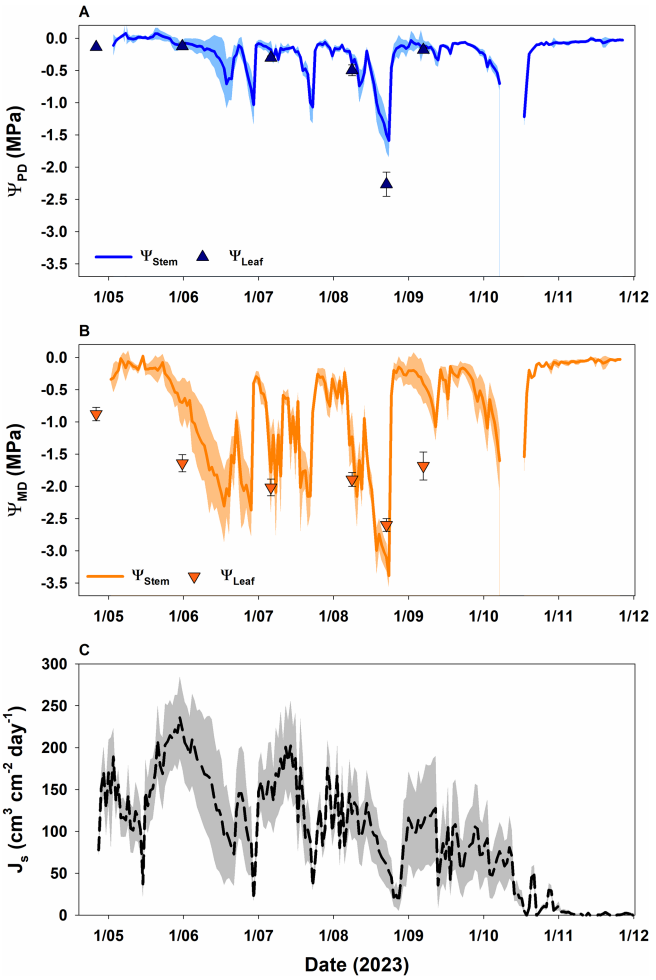

FIGURE 2 | Predawn (A), midday (B) stem water potential (Ψ_{Stem}) and sap flux density (J_s) with 95% confidence interval from May to September 2023. In Panels A and B, leaf water potentials (Ψ_{Leaf}) ±1 SE are shown as triangles. Ψ_{Stem} measurements were conducted with FloraPulse stem water potential sensors. Ψ_{Leaf} was measured with the Scholander pressure chamber. In September, logger failure caused a data loss of 2 weeks for Ψ_{Stem}.

Ψ_{Stem}, e.g., also with a distinct second dry-down period in late August and J_s close to 0 $cm^3\,cm^{-2}\,day^{-1}$ (Figure 2C). After leaf senescence starting in mid-October, J_s ceased in early November, in agreement with high Ψ_{Stem}.

3.3 | Comparison of Stem and Leaf Water Potential

The agreement between Ψ_{Leaf} and Ψ_{Stem} was reasonable however differed between Ψ_{PD} and Ψ_{MD} (Figure 3, Figure S2–S6). For Ψ_{PD}, the relationship of both parameters was highly significant ($p < 0.001$, $R^2_c = 0.98$). Ψ_{Leaf} was slightly lower than Ψ_{Stem}, which was especially evident in August 2023 (Figure 2A), leading to a slope of the regression in Figure 3A of 1.49 ± 0.05 MPa MPa^{-1}. Interestingly, the largest discrepancy between Ψ_{Leaf} and Ψ_{Stem} was measured when VPD values did not drop below 0.19 kPa in the night (23 August), which led to nocturnal sap flow of *C. betulus* at the time of predawn measurements of Ψ_{Leaf} (Figure S5).

The relationship of Ψ_{Leaf} and Ψ_{Stem} during midday was more variable (Figure 3B) but still highly significant ($p < 0.001$, $R^2_c = 0.71$). Interestingly, the slope of the regression was below 1 (0.38 ± 0.06 MPa MPa^{-1}). Potentially, this was due to missing Ψ_{Leaf} measurements above −1.50 MPa and missing measurements on cloudy days. Thus, the relationship of Ψ_{Leaf} and Ψ_{Stem} presented here might only be reliable for the given measurement range on sunny days and might need validation for higher Ψ_{MD} values.

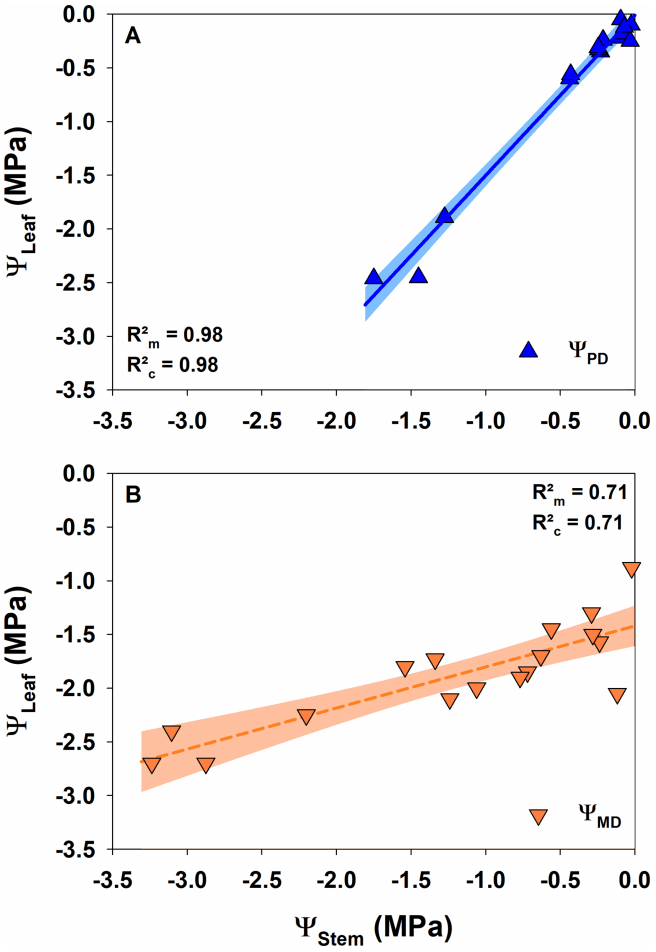

FIGURE 3 | Regression (linear mixed-effect model) of stem water potential (Ψ_{Stem}) and leaf water potential (Ψ_{Leaf}) for predawn (A) and midday conditions (B) with marginal (R^2_m) and conditional R^2 (R^2_c).

Diurnal courses were measured at the end of the study period, when Ψ_{PD} were high, and indicated a very good agreement between Ψ_{Leaf} and Ψ_{Stem} ($R^2 = 0.81$–0.86), albeit with three specific differences: (1) Ψ_{Leaf} was significantly lower and showed a stronger diurnal amplitude than Ψ_{Stem} (Figure 4A,C,E), (2) there was a strong lag between Ψ_{Leaf} and Ψ_{Stem} ranging from 100 to 220 min, (3) and the relationship of Ψ_{Leaf} and Ψ_{Stem} differed between trees (Figure 4B,D,F). As Ψ_{Leaf} and Ψ_{Stem} were measured on different parts of the trees, and trees had different positions in the forest canopy regarding environmental conditions, such as light, we further evaluated Ψ_{Stem} with data of sap flow sensors installed in the stem and environmental conditions.

3.4 | Response of Stem Water Potential to Environmental Parameters

Besides comparing Ψ_{Stem} with Ψ_{Leaf}, we evaluated the relationship of Ψ_{Stem} with the concurrently measured environmental parameters T_{air}, VPD_{max} and VWC (Figure 5). For Ψ_{PD}, there was a weak tendency of decreasing values with rising T_{air} and VPD_{max} (Figure 5A,C). *C. betulus* mainly responded to soil drying (VWC, $R_c^2 = 0.59$) with a drop of Ψ_{PD}, especially when VWC declined below ~8% (Figure 5E). Ψ_{MD} of *C. betulus* decreased simultaneously with increasing VPD_{max} ($R^2_c = 0.59$, $p < 0.001$), T_{air} ($R^2_c = 0.48$, $p < 0.001$) and decreasing VWC ($R^2_c = 0.74$) (Figure 5B,D,F). Thus, plants reacted strongly to a combination of drier and hotter conditions.

3.5 | Relationship of Sap Flow and Stem Water Potential

J_s and Ψ_{Stem} variations showed opposing diurnal courses for all measured trees, and agreed in dynamics (Figure 6). While J_s increased strongly between 7 AM and 3 PM (CEST, on average), Ψ_{Stem} decreased simultaneously. Between 3 PM and 7 AM (CEST, on average), this pattern was reversed. However, the relationship of the two parameters was different in the two time periods (Figure 6A,C,E), indicating a hysteresis (Figure 6B,D,F). With increasing J_s, Ψ_{Stem} simultaneously decreased; however, maximum J_s was reached, 100–120 min before minimum Ψ_{Stem} occurred. After maximum J_s was reached, J_s decreased quickly and approached values of $< 0.5\,cm^3\,cm^{-2}$ already in the early evening. Yet, Ψ_{Stem} recovered significantly slower, only approaching initial values after midnight (Figure 6A,C,E).

Seasonally, the relationship between sum of J_s and mean Ψ_{Stem} illustrated that these two parameters were also not linearly related, but rather that there was a linear relationship with maximum J_s (Figure 7A) under water limitation. With a drop of 1 MPa in mean daytime Ψ_{Stem}, the maximum daily J_s decreased by 82.0 ± 3.9 $cm^3\,cm^{-2}\,day^{-1}$ ($p < 0.001$, $R^2 = 0.96$). On days, where J_s did not reach the maximum J_s depicted by the regression line, potentially other (environmental) factors than Ψ_{Stem} (co-)limited

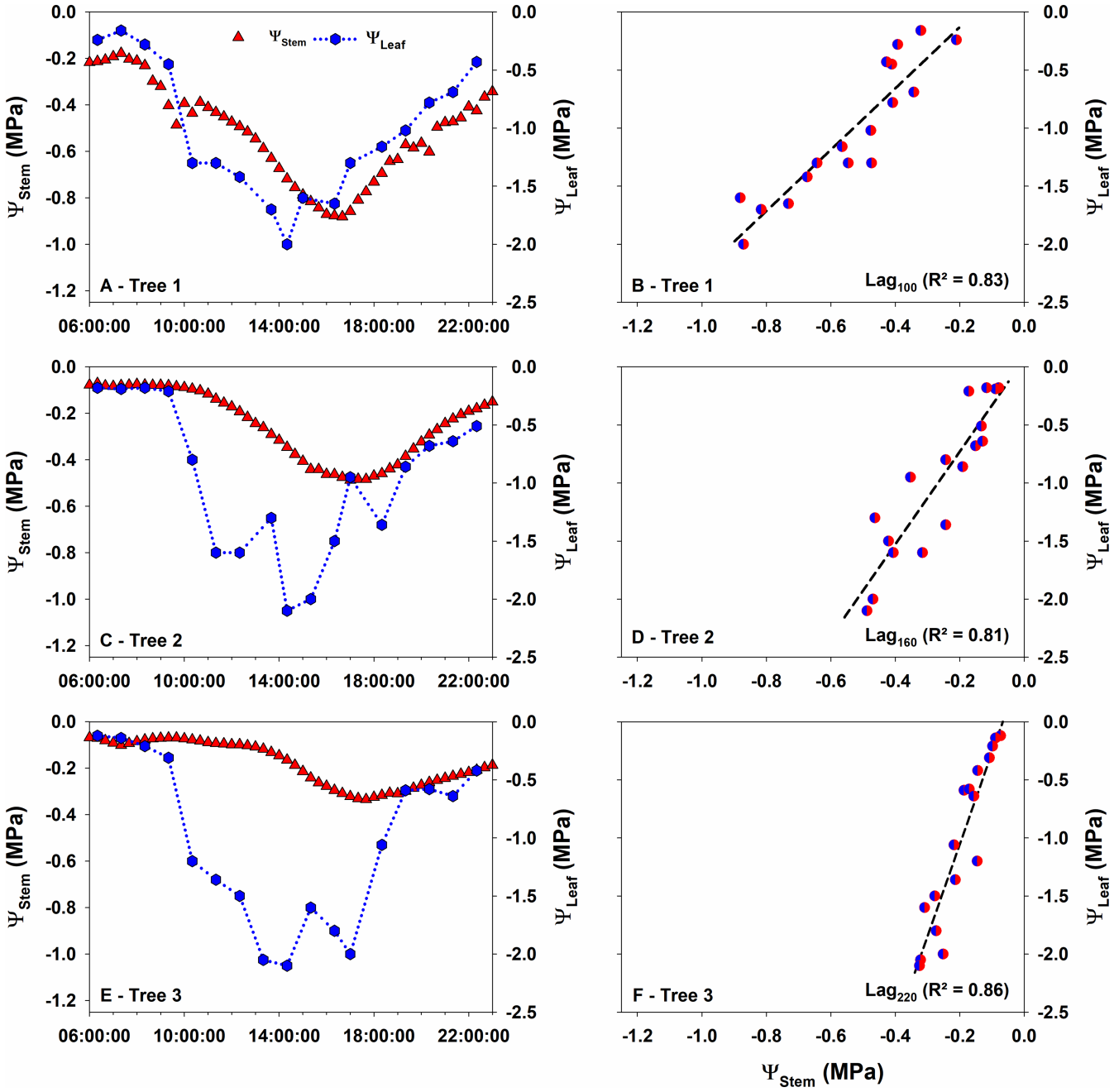

FIGURE 4 | Diurnal course of stem water potential (Ψ_{Stem}) and leaf water potential (Ψ_{Leaf}) on 7 September for all measured trees (A, C, E) and the regression between Ψ_{Stem} and Ψ_{Leaf} with R^2 including a lag of 100–220 min (B, D, F). Note the different scales for Ψ_{Stem} and Ψ_{Leaf}.

J_s. Maximum J_s was reached at Ψ_{Stem} values of ~−0.4 MPa (Figure 7A).

The most significant environmental factor impacting J_s was VPD_{mean}, albeit with different relationships depending on VWC (Figure 7C). Under high VWC (>13%), J_s strongly increased ($p < 0.001$) with rising VPD_{mean} ($R^2_c = 0.93$). Under low VWC (<13%), J_s initially increased with rising VPD_{mean} ($p < 0.001$, $R^2_c = 0.61$), but at lower rates than under high VWC. At a VPD_{mean} of ~1.5 kPa, J_s started to decline, indicating a co-limitation by low soil water resources. Indeed, J_s declined after the VWC threshold of approximately 13% was reached (Figure 7D). In general, J_s also increased with rising T_{air}; however, as VPD_{mean} is known to be a stronger predictor for J_s than T_{air}, no regression was fitted (Figure 7B).

4 | Discussion

In general, seasonal predawn stem water potentials obtained for *C. betulus* agreed well with traditional Scholander pressure chamber measurements (Ψ_{Leaf}, with minor deviations), sap flow dynamics and environmental conditions. We identified some patterns, which require further discussion and might hint at potential inaccuracies or limitations of the microtensiometer, such as discrepancies of Ψ_{Stem} and Ψ_{Leaf} during daytime in absolute

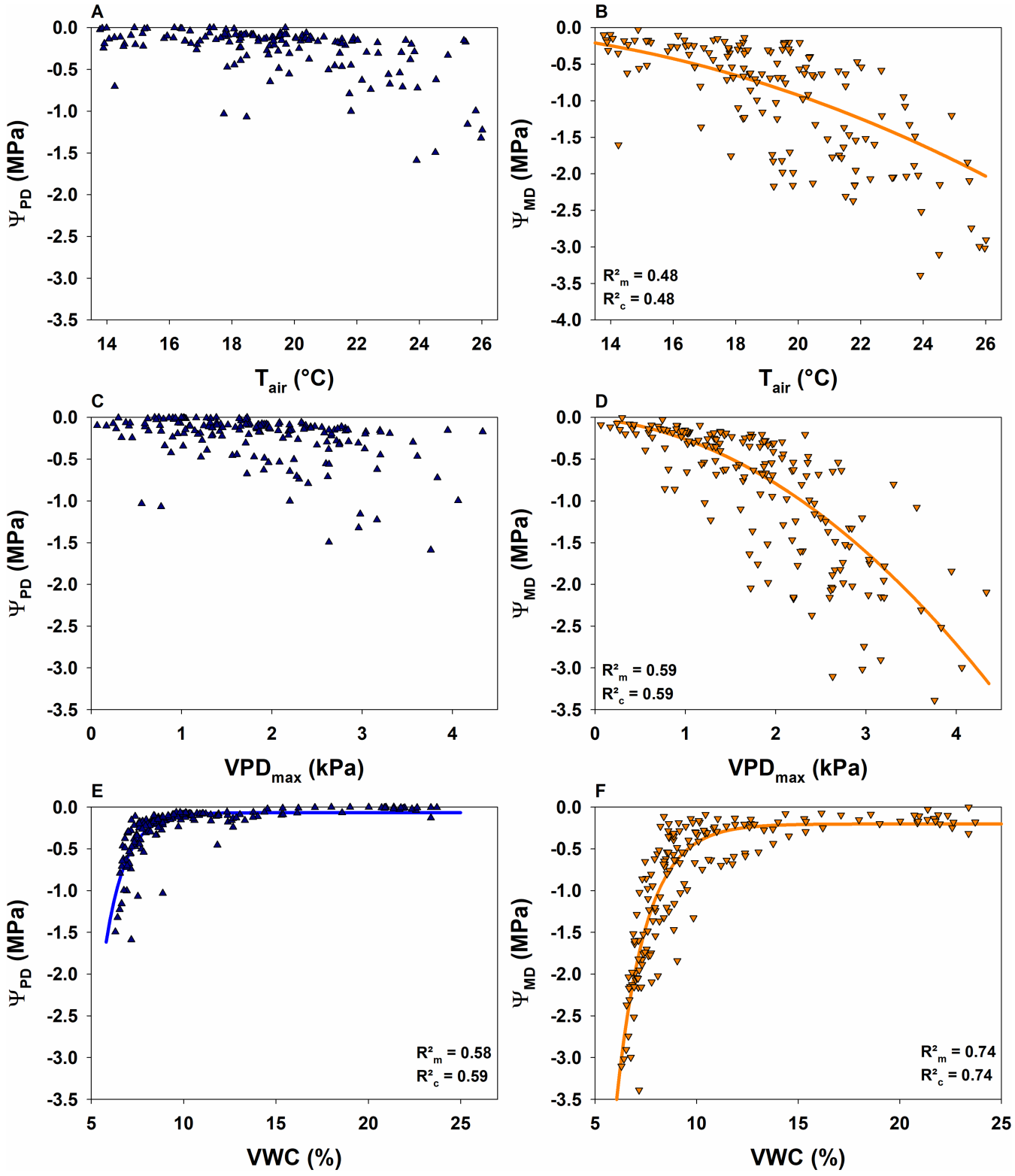

FIGURE 5 | Relationship of Ψ_{Stem} with mean daily air temperature (T_{air}) (A, B), maximum daily vapour pressure deficit (VPD_{max}) (C, D) and mean daily volumetric soil water content (VWC) (E, F) or predawn (A, C, E) and midday conditions (B, D, F). Values after October were not considered due to leaf senescence. R^2_m refers to the marginal R^2, R^2_c to the conditional R^2 of the applied linear mixed-effect model in Panels B, D, E and F.

values, variability and magnitude. Yet, we demonstrate that continuous Ψ_{Stem} data in combination with J_s hold a high potential in elucidating important links between the two parameters and interrelated processes to confront the water potential information gap (Novick et al. 2022).

4.1 | Ψ_{Stem} Is Buffered Compared to Ψ_{Leaf}

During the day, a significant water potential gradient is building up within the plant, which drives plant water fluxes (e.g., Larcher 1994). As we measured Ψ_{Stem} at ~1 m and Ψ_{Leaf} at

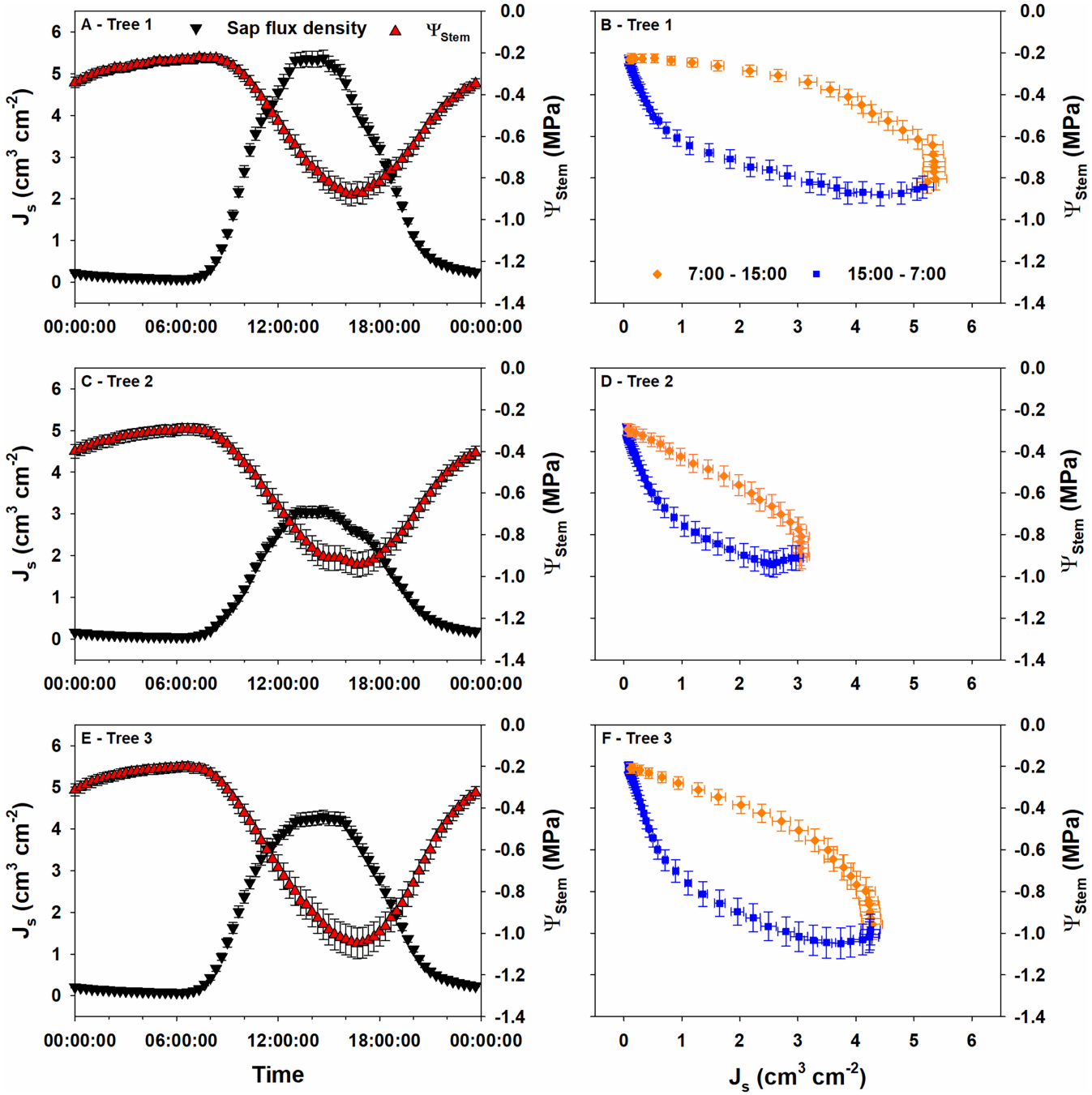

FIGURE 6 | Average diurnal course of sap flux density (J_s) ±1 SE and stem water potential (Ψ_{Stem}) ± 1 SE for all measured trees (A, C, E) and relationship of J_s ±1 SE and Ψ_{Stem} ±1 SE for all measured trees (B, D, F) between May and October 2023. Values after October were not considered due to leaf senescence.

~8–10 m height, differences in absolute values, magnitude and variability of Ψ are to be expected during the day, and need to be accounted for. Thus, the differences in midday/diurnal Ψ_{Stem} and Ψ_{Leaf} measurements (Figure 2B, Figure 4) can in part be associated to lower Ψ_{Leaf} in sunlit leaves and the different positions of (8 and 1 m) in the canopy. Nevertheless, the large mismatch during diurnal courses, particularly in the afternoon, could also hint at potential limitations of the new microtensiometer in accurately capturing daytime water potentials, as also reported by Blanco and Kalcsits (2023). Yet, it is known that Ψ in the stem is buffered compared to Ψ in leaves, express higher Ψ and a lower diurnal variability (Jarvis 1976; Larcher 1994; Scholz et al. 2007; Nikinmaa, Sievänen, and Hölttä 2014). Ψ_{Leaf} measurements in the tree crown are highly variable and reflect the diverse, often fast changing microclimatic conditions, such as light levels (e.g., Burgess and Dawson 2008), while Ψ_{Stem} is, similar to J_s at the stem base, an integrative signal of the tree's response, comprising the response of all branches and leaves in the tree crown. Thus, it is reasonable to assume that the measured Ψ_{Stem} values are reliable in capturing diurnal and seasonal Ψ dynamics, although with two restrictions: (1) The relationship of Ψ_{Stem} and Ψ_{Leaf} for midday conditions shown in Figure 3B might only be valid for sunny days, as we did not measure Ψ_{Leaf} on cloudy days. (2) On 23 August, Ψ_{Stem} was lower than Ψ_{Leaf} (Figure S5), which

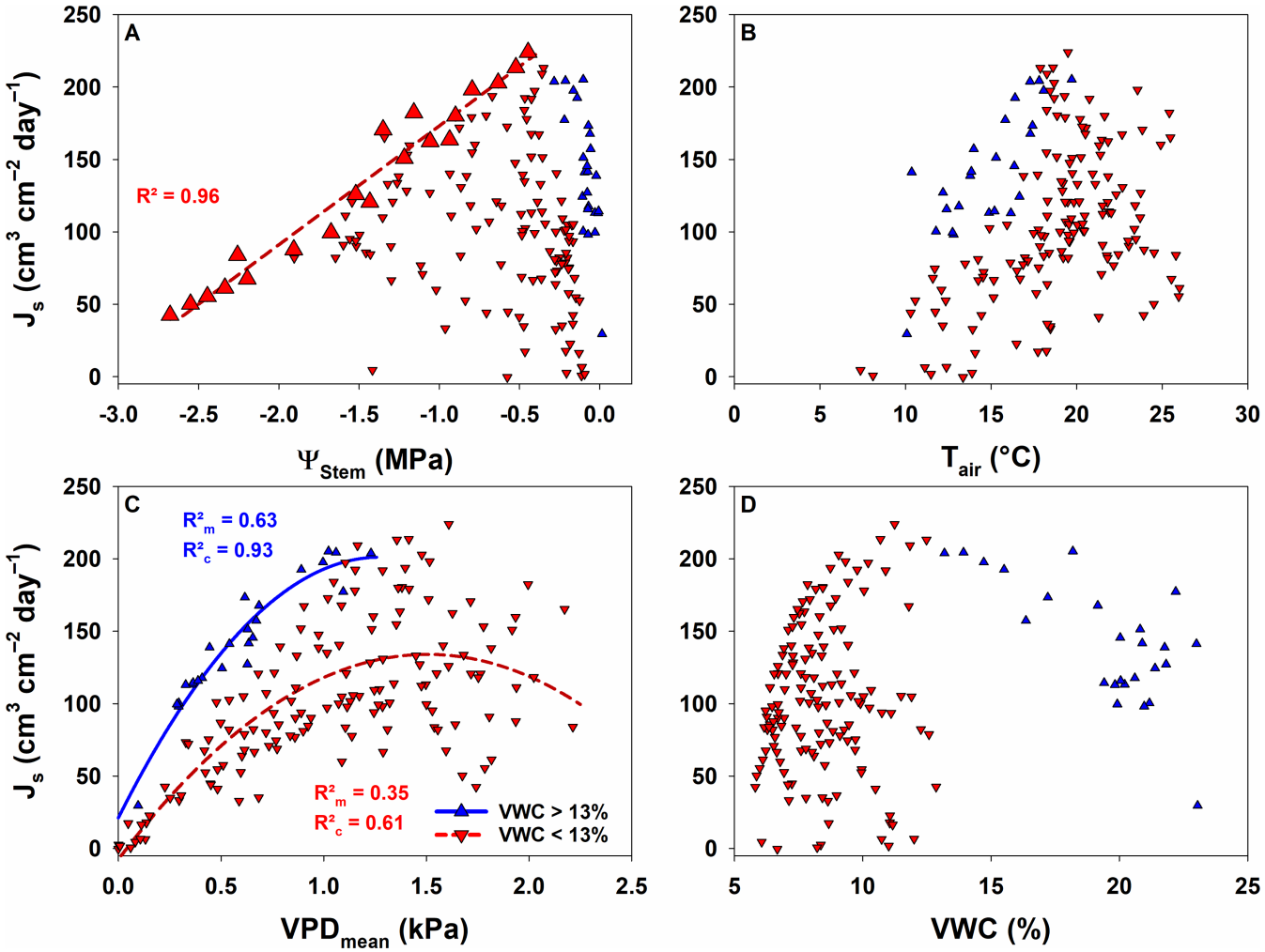

FIGURE 7 | Relationship of daily sap flux density (J_s) with mean daily stem water potential (Ψ_{Stem}) (A), mean daily air temperature (T_{air}), mean daily vapour pressure deficit (VPD_{mean}) with quadratic regression (C) and mean daily volumetric soil water content (VWC) (D). Data points in A–D are separated into periods with VWC higher (blue triangles) and VWC lower (red triangles) than the threshold of 13%. Large points in Panel A were used for a linear regression between J_s and Ψ_{Stem} to determine the maximum J_s at a given Ψ_{Stem}. R^2_m refers to the marginal R^2, R^2_c to the conditional R^2 of the applied linear mixed-effect model in Panel C. Data were only used during daytime between sunrise and sunset.

might question the accuracy of the stem water potential sensor close to its operating limit given by the manufacturer (−3.5 MPa). Users should be aware of this limit in measurement range of the microtensiometer and filter the data accordingly.

While some inaccuracies between Ψ_{Stem} and Ψ_{Leaf} were evident in the diurnal measurements, novel microtensiometers were accurately capturing water potentials during predawn conditions (Figure 2A, Figure 4). This is in line with the theory that plant water potential equilibrates with soil water potential during the night, when water reserves are replenished (Hinckley, Lassoie, and Running 1978; Richter 1997). This was the case during most of the study periods; however, during one drier period in August 2023, predawn Ψ_{Leaf} was 0.6–1.0 MPa lower than Ψ_{Stem} (Figure S5), which may indicate an incomplete refilling of tree water reserves. Thus, under drought conditions, sampling height should be considered as important factor, as a larger sampling height might yield more negative water potential values, which could be further exacerbated by progressing drought conditions. Such predawn disequilibrium has also been observed under non-drought conditions (Donovan, Linton, and Richards 2001; Donovan, Richards, and Linton 2003), and has been attributed to the occurrence of nocturnal transpiration (Donovan, Richards, and Linton 2003; Kavanagh, Pangle, and Schotzko 2007; Kangur et al. 2021) and high nocturnal VPD (Kangur, Kupper, and Sellin 2017). Our data suggests that predawn disequilibrium actually occurred during nights of high VPD and led to the observed discrepancy of Ψ_{Stem} and Ψ_{Leaf} under dry conditions. Thus, Ψ_{Leaf} should be measured over a large range of predawn conditions (including severe drought) to verify Ψ_{Stem} measurements and to account for predawn disequilibrium.

4.2 | The Hysteresis of Diurnal Stem Water Potential and Sap Flow Raises the Question of Stem Capacitance

The occurrence of hysteresis in plant water relations is well known and has been observed for water fluxes in stem and needles/leaves (e.g., Larcher 1994), xylem diameter variations and sap flow (e.g., Sevanto et al. 2008) and stem water potential and sap flow (e.g., Stöhr and Lösch 2004). The latter two

have been connected to the usage of stored water in stem and bark, which can be exchanged with and released into the transpiration stream (Wullschleger, Meinzer, and Vertessy 1998; Zweifel, Item, and Häsler 2001; Scholz et al. 2011). This capacitive discharge can buffer daily variations in xylem tension, preventing embolism and hydraulic dysfunction (Scholz et al. 2011; McCulloh et al. 2019). For example, higher stem capacitance led to less negative leaf Ψ_{MD} in tropical species (Scholz et al. 2007), and allowed *Pinus halepensis* to maintain a sufficient hydraulic safety margin during the dry season (Preisler et al. 2022). Thus, it is likely that the hysteresis of Ψ_{Stem} and J_s in *C. betulus* was caused by the release of stored water to buffer fluctuations in xylem tension. Recently, Leuschner et al. (2024) demonstrated that 10.5%–13.0% of the daily water consumption of *C. betulus* actually originated from stem water storage.

Likewise, the lag of Ψ_{Stem} and Ψ_{Leaf} during our diurnal measurements (Figure 4) was potentially caused by similar mechanisms. As measurements were conducted in a period of high Ψ_{PD}, stem water reserves were most likely filled, leading to only minor variations in xylem tension. Low Ψ_{Leaf} at the same time point towards an increasing physiological activity, also evident from increasing J_s, after recovery rainfall at the beginning of September. Especially for Tree 3 (Figure 4E), the question arises, if Ψ_{Stem} was representative for Ψ_{Leaf} on this day, as only a minor diurnal variation (~0.20 MPa) in Ψ_{Stem} was observed, although Ψ_{Leaf} dropped to values < −2.0 MPa. Either Ψ_{Stem} measurements were erroneous, or there is the possibility of within species tree individual capacitance differences, similar to between species differences in capacitance (Scholz et al. 2007; Scholz et al. 2011). In conclusion, the measurement day in September was not ideal, and the diurnal variation of Ψ_{Stem} and Ψ_{Leaf} should also be measured during dry periods to better establish a relationship between the two parameters over a larger range of environmental conditions. Additionally, stem diameter variations and tree water deficit (Zweifel et al. 2016), calculated via dendrometers, may be a promising approach to further evaluate Ψ_{Stem} (and vice versa) (cf. Dietrich, Zweifel, and Kahmen 2018; Gleason et al. 2024; Ziegler et al. 2024), as xylem tension and stem diameter changes are closely related (Irvine and Grace 1997).

4.3 | Stem Water Potential Determines Maximum Plant Water Fluxes

Both, Ψ_{Stem} and J_s, responded similarly to environmental stressors, mirroring the relationship of sap flow and VPD/VWC under edaphic and atmospheric drought (e.g., Sánchez-Costa, Poyatos, and Sabaté 2015; Haberstroh et al. 2022a). While Szatniewska et al. (2022) observed that VPD is a stronger predictor of J_s than VWC for *C. betulus*, we found a co-limitation of J_s by both factors under low soil moisture. This co-limitation is well known (Granier et al. 2007; Haberstroh et al. 2022a), but only occurs once a certain threshold of soil moisture is exceeded. Most likely, soil moisture levels in Szatniewska et al. (2022) did not drop to critical levels, which might explain the differences to our study. Moreover, during these periods of limited soil water resources, we observed that the maximum J_s of *C. betulus* declined linearly with declining Ψ_{Stem} (Figure 7A) (cf. Cruiziat, Cochard, and Améglio 2002). During water limitation, water potentials in plants, such as *C. betulus* (Li et al. 2016), drop, which could potentially trigger stomatal closure and, thus, reduce J_s. However, J_s started to decline at values of Ψ_{Stem} of −0.4 MPa, which is significantly higher than critical thresholds for *C. betulus*, where trees lose 12% (Ψ_{12} = −3.3 MPa, Leuschner et al. 2024) or 50% (Ψ_{50} = −3.75–4.3 MPa; Herbette and Cochard 2010; Li et al. 2016) of their hydraulic conductivity. Thus, the decline in J_s (and stomatal conductance) was most likely triggered by a different mechanism, such as the loss of soil or root hydraulic conductivity, which may induce stomatal closure under drought, rather than xylem cavitation (Carminati and Javaux 2020; Abdalla et al. 2022; Wankmüller et al. 2024). Continuous Ψ_{Stem} data in combination with J_s might provide a way forward to elucidate these patterns in more detail (McCulloh et al. 2019).

5 | Conclusion

Stem water potentials obtained continuously with microtensiometers offer a high potential for ecophysiological and ecohydrological stress research, if applicable in other important tree species. In combination with ecophysiological measures, such as sap flow or tree water deficits, tree stress can be detected and investigated dynamically. Continuous stem water potential data further have the potential to improve modelling approaches of tree drought response and mortality events (Steppe 2018; Hartmann et al. 2018; Novick et al. 2022) and allow for a better investigation of stem capacitance, as data on capacitance and water potential, measured on the same location, are scarce, but pivotal for capacitance studies (Scholz et al. 2011). Beside these fundamental findings on processes, the effort to obtain data changes drastically, as continuous datasets can be collected without time- and labour-consuming Scholander pressure chamber measurements.

The data presented here are promising, although stem water potential sensors need to be rigorously evaluated for every species. In particular, the relationship of Ψ_{Stem} and Ψ_{Leaf} data requires further assessments in different conditions, as we found an offset in Ψ_{Stem} and Ψ_{Leaf} under midday conditions. Ψ_{Stem} can provide a more integrative measure of stress that includes the response to environmental factors of an entire forest canopy, while Ψ_{Leaf} is additionally dependent on the diverse, fast changing environmental conditions in the tree crown, representing a specific part of the canopy. In conclusion, continuous stem water potential data have a high potential in advancing our knowledge about tree and forest drought responses and confront the water potential information gap (Novick et al. 2022), especially in combination with sap flow measurements.

Acknowledgements

We thank Thomas Plapp, Dirk Redepennig, Dirk Schindler and Matthias Zeeman (Chair of Environmental Meteorology, University of Freiburg) and Thomas Seifert and Benjamin Gebert (Chair of Forest Growth and Dendroecology, University of Freiburg) for site logistics data management, and support. We acknowledge funding of the SFB1537 (ECOSENSE) (Werner et al. 2024) and support by the Integrated Carbon Observation System (ICOS, Site DE-Har) for processing and managing the long-term environmental data. Open Access funding enabled and organized by Projekt DEAL.

Conflicts of Interest

The authors declare no conflicts of interest.

Data Availability Statement

The data that support the findings of this study are available from the corresponding author upon reasonable request. Meteorological data (in-canopy-air temperature and above-canopy precipitation for 2023) are available from Zenodo (Christen, Plapp, and Schindler 2024a, 2024b).

References

Abdalla, M., M. A. Ahmed, G. Cai, et al. 2022. "Stomatal Closure During Water Deficit Is Controlled by Below-Ground Hydraulics." *Annals of Botany* 129: 161–170. https://doi.org/10.1093/aob/mcab141.

Bartoń, K. 2022. MuMIn: Multi-Model Inference. R Package Version 1.47.1, https://CRAN.R-project.org/package=MuMIn.

Blanco, V., and L. Kalcsits. 2023. "Long-Term Validation of Continuous Measurements of Trunk Water Potential and Trunk Diameter Indicate Different Diurnal Patterns for Pear Under Water Limitations." *Agricultural Water Management* 281: 108257. https://doi.org/10.1016/j.agwat.2023.108257.

Blanco, V., and L. Kalcsits. 2024. "Relating Microtensiometer-Based Trunk Water Potential With Sap Flow, Canopy Temperature, and Trunk and Fruit Diameter Variations for Irrigated 'Honeycrisp' Apple." *Frontiers in Plant Science* 15: 1393028. https://doi.org/10.3389/fpls.2024.1393028.

Bourbia, I., C. Lucani, M. R. Carins-Murphy, A. Gracie, and T. J. Brodribb. 2023. "In Situ Characterisation of Whole-Plant Stomatal Responses to VPD Using Leaf Optical Dendrometry." *Plant, Cell & Environment* 46: 3273–3286. https://doi.org/10.1111/pce.14658.

Brandes, E., J. Wenninger, P. Koeniger, et al. 2007. "Assessing Environmental and Physiological Controls Over Water Relations in a Scots Pine (*Pinus sylvestris* L.) Stand Through Analyses of Stable Isotope Composition of Water and Organic Matter." *Plant, Cell and Environment* 30: 113–127. https://doi.org/10.1111/j.1365-3040.2006.01609.x.

Brodribb, T. K. 2009. "Xylem Hydraulic Physiology: The Functional Backbone of Terrestrial Plant Productivity." *Plant Science* 177: 245–251. https://doi.org/10.1016/j.plantsci.2009.06.001.

Burgess, S. S. O., M. A. Adams, N. C. Turner, et al. 2001. "An Improved Heat Pulse Method to Measure Low and Reverse Rates of Sap Flow in Woody Plants." *Tree Physiology* 21: 589–598. https://doi.org/10.1093/treephys/21.9.589.

Burgess, S. S. O., and T. E. Dawson. 2008. "Using Branch and Basal Trunk Sap Flow Measurements to Estimate Whole-Plant Water Capacitance: A Caution." *Plant and Soil* 305: 5–13. https://doi.org/10.1007/s11104-007-9378-2.

Carminati, A., and M. Javaux. 2020. "Soil Rather Than Xylem Vulnerability Controls Stomatal Response to Drought." *Trends in Plant Science* 25: 868–880. https://doi.org/10.1016/j.tplants.2020.04.003.

Choat, B., T. J. Brodribb, C. R. Brodersen, R. A. Duursma, R. López, and B. Medlyn. 2018. "Triggers of Mortality Under Drought." *Nature* 558: 531–539. https://doi.org/10.1038/s41586-018-0240-x.

Christen, A., T. Plapp, and D. Schindler. 2024a. *In-Canopy Air Temperature Measurements at Hartheim Forest Research Site (DE-Har) From 2023-01-01 to 2023-12-31 [L2] [Dataset]*. Zenodo. https://doi.org/10.5281/zenodo.13900204.

Christen, A., T. Plapp, and D. Schindler. 2024b. *Above-Canopy Precipitation Measurements at Hartheim Forest Research Site (DE-Har) From 2023-01-01 to 2023-12-31 [L2] [Dataset]*. Zenodo. https://doi.org/10.5281/zenodo.14269892.

Cruiziat, P., H. Cochard, and T. Améglio. 2002. "Hydraulic Architecture of Trees: Main Concepts and Results." *Annals of Forest Science* 59: 723–752. https://doi.org/10.1051/forest:2002060.

Dietrich, L., R. Zweifel, and A. Kahmen. 2018. "Daily Stem Diameter Variations Can Predict the Canopy Water Status of Mature Temperate Trees." *Tree Physiology* 38: 941–952. https://doi.org/10.1093/treephys/tpy023.

Donovan, L. A., M. J. Linton, and J. H. Richards. 2001. "Predawn Plant Water Potential Does Not Necessarily Equilibrate With Soil Water Potential Under Well-Watered Conditions." *Oecologia* 129: 328–335. https://doi.org/10.1007/s004420100738.

Donovan, L. A., J. H. Richards, and M. J. Linton. 2003. "Magnitude and Mechanisms of Disequilibrium Between Predawn Plant and Soil Water Potentials." *Ecology* 84: 463–470. https://doi.org/10.1890/0012-9658(2003)084[0463:MAMODB]2.0.CO;2.

Gleason, S. M., J. J. Stewart, B. Allen, et al. 2024. "Development and Application of an Inexpensive Opensource Dendrometer for Detecting Xylem Water Potential and Radial Stem Growth at High Spatial and Temporal Resolution." *AoB Plants* 16: plae009. https://doi.org/10.1093/aobpla/plae009.

González, L., A. Huber, R. Gao, et al. 2022. "Using Micro-Tensiometers to Manage Water Stress to Maximize Fruit Size of Apple Orchards." *Acta Horticulturae* 1373: 113–120. https://doi.org/10.17660/ActaHortic.2023.1373.16.

Granier, A., M. Reichstein, N. Bréda, et al. 2007. "Evidence for Soil Water Control on Carbon and Water Dynamics in European Forests During the Extremely Dry Year: 2003." *Agricultural and Forest Meteorology* 143: 123–145. https://doi.org/10.1016/j.agrformet.2006.12.004.

Guo, J. S., K. R. Hultine, G. W. Koch, H. Kropp, and K. Ogle. 2020. "Temporal Shifts in Iso/Anisohydry Revealed From Daily Observations of Plant Water Potential in a Dominant Desert Shrub." *New Phytologist* 225: 713–726. https://doi.org/10.1111/nph.16196.

Haberstroh, S., R. Lobo-do-Vale, M. Caldeira, M. Dubbert, M. Cuntz, and C. Werner. 2022a. "Plant Invasion Modifies Isohydricity of Mediterranean Tree Species." *Functional Ecology* 36: 2384–2398. https://doi.org/10.1111/1365-2435.14126.

Haberstroh, S., C. Werner, M. Grün, et al. 2022b. "Central European 2018 Hot Drought Shifts Scots Pine Forest to Its Tipping Point." *Plant Biology* 24: 1186–1197. https://doi.org/10.1111/plb.13455.

Hartmann, H., C. F. Moura, W. R. L. Anderegg, et al. 2018. "Research Frontiers for Improving Our Understanding of Drought-Induced Tree and Forest Mortality." *New Phytologist* 218: 15–28. https://doi.org/10.1111/nph.15048.

Herbette, S., and H. Cochard. 2010. "Calcium Is a Major Determinant of Xylem Vulnerability to Cavitation." *Plant Physiology* 153: 1932–1939. https://doi.org/10.1104/pp.110.155200.

Hinckley, T. M., J. P. Lassoie, and S. W. Running. 1978. "Temporal and Spatial Variations in the Water Status of Forest Trees." *Forest Science* 24: a0001–z0001. https://doi.org/10.1093/forestscience/24.s1.a0001.

Irvine, J., and J. Grace. 1997. "Continuous Measurements of Water Tensions in the Xylem of Trees Based on the Elastic Properties of Wood." *Planta* 202: 455–461. https://doi.org/10.1007/s004250050149.

Jarvis, P. G. 1976. "The Interpretation of the Variations in Leaf Water Potential and Stomatal Conductance Found in Canopies in the Field." *Philosophical Transactions of the Royal Society of London. Series B, Biological Sciences* 273: 593–610. https://doi.org/10.1098/rstb-1976.0035.

Kangur, O., P. Kupper, and A. Sellin. 2017. "Predawn Disequilibrium Between Soil and Plant Water Potentials in Light of Climate Trends Predicted for Northern Europe." *Regional Environmental Change* 17: 2159–2168. https://doi.org/10.1007/s10113-017-1183-8.

Kangur, O., K. Steppe, J. D. M. Schreel, J. S. von der Crone, and A. Sellin. 2021. "Variation in Nocturnal Stomatal Conductance and Development

of Predawn Disequilibrium Between Soil and Leaf Water Potentials in Nine Temperate Deciduous Tree Species." *Functional Plant Biology* 48: 483–492. https://doi.org/10.1071/FP20091.

Kavanagh, K. L., R. Pangle, and A. D. Schotzko. 2007. "Nocturnal Transpiration Causing Disequilibrium Between Soil and Stem Predawn Water Potential in Mixed Conifer Forests of Idaho." *Tree Physiology* 27: 621–629. https://doi.org/10.1093/treephys/27.4.621.

Kinzinger, L., J. Mach, S. Haberstroh, et al. 2024. "Interaction Between Beech and Spruce Trees in Temperate Forests Affects Water Use, Root Water Uptake Pattern and Canopy Structure." *Tree Physiology* 44: tpad144. https://doi.org/10.1093/treephys/tpad144.

Larcher, W. 1994. *Ökophysiologie der Pflanzen*. 5th ed. Stuttgart, Germany: Verlag Eugen Ulmer Stuttgart.

Lasko, A. M., M. Santiago, and A. D. Stroock. 2022. "Monitoring Stem Water Potential With an Embedded Microtensiometer to Inform Irrigation Scheduling in Fruit Crops." *Horticulturae* 8: 1207. https://doi.org/10.3390/horticulturae8121207.

Leuschner, C., S. Fuchs, P. Wedde, E. Rüther, and B. Schuldt. 2024. "A Multi-Criteria Drought Resistance Assessment of Temperate *Acer, Carpinus, Fraxinus, Quercus*, and *Tilia* Species." *Perspectives in Plant Ecology, Evolution and Systematics* 62: 125777. https://doi.org/10.1016/j.ppees.2023.125777.

Li, S., M. Feifel, Z. Karimi, B. Schuldt, B. Choat, and S. Jansen. 2016. "Leaf Gas Exchange Performance and the Lethal Water Potential of Five European Species During Drought." *Tree Physiology* 36: 179–192. https://doi.org/10.1093/treephys/tpv117.

Mantova, M., S. Herbette, H. Cochard, and J. M. Torres-Ruiz. 2022. "Hydraulic Failure and Tree Mortality: From Correlation to Causation." *Trends in Plant Science* 27: 335–345. https://doi.org/10.1016/j.tplants.2021.10.003.

Marshall, D. C. 1958. "Measurement of Sap Flow in Conifers by Heat Transport." *Plant Physiology* 33: 385–396. https://doi.org/10.1104/pp.33.6.385.

Martín-Gómez, P., U. Rodríguez-Robles, J. Ogée, et al. 2023. "Contrasting Stem Water Uptake and Storage Dynamics of Water-Saver and Water-Spender Species During Drought and Recovery." *Tree Physiology* 43: 1290–1306. https://doi.org/10.1093/treephys/tpad032.

McCulloh, K. A., J.-C. Domec, D. M. Johnson, D. D. Smith, and F. C. Meinzer. 2019. "A Dynamic Yet Vulnerable Pipeline: Integration and Coordination of Hydraulic Traits Across Whole Plants." *Plant, Cell & Environment* 42: 2789–2807. https://doi.org/10.1111/pce.13607.

McDowell, N. G. 2011. "Mechanisms Linking Drought, Hydraulics, Carbon Metabolism, and Vegetation Mortality." *Plant Physiology* 155: 1051–1059. https://doi.org/10.1104/pp.110.170704.

Miguez, F. 2023. Nlraa: Nonlinear Regression for Agricultural Applications. R Package Version 1.9.3, https://CRAN.R-project.org/package=nlraa.

Nikinmaa, R., R. Sievänen, and T. Hölttä. 2014. "Dynamics of Leaf Gas Exchange, Xylem and Phloem Transport, Water Potential and Carbohydrate Concentration in a Realistic 3-D Model Tree Crown." *Annals of Botany* 114: 653–666. https://doi.org/10.1093/aob/mcu068.

Novick, K. A., D. L. Ficklin, D. Baldocchi, et al. 2022. "Confronting the Water Potential Information Gap." *Nature Geoscience* 15: 158–164. https://doi.org/10.1038/s41561-022-00909-2.

Pagay, V. 2022. "Evaluating a Novel Microtensiometer for Continuous Trunk Water Potential Measurements in Field-Grown Irrigated Grapevines." *Irrigation Science* 40: 45–54. https://doi.org/10.1007/s00271-021-00758-8.

Philip, J. R. 1966. "Plant Water Relations: Some Physical Aspects." *Annual Review of Plant Physiology* 17: 245–268.

Pinheiro, J., D. Bates, and R Core Team. 2023. Nlme: Linear and Nonlinear Mixed Effects Models. R Package Version 3.1–163, https://CRAN.R-project.org/package=nlme.

Preisler, Y., T. Hölttä, J. M. Grünzweig, et al. 2022. "The Importance of Tree Internal Water Storage Under Drought Conditions." *Tree Physiology* 42: 771–783. https://doi.org/10.1093/treephys/tpab144.

R Core Team. 2022. *R: A Language and Environment for Statistical Computing*. Vienna, Austria: R Foundation for Statistical Computing. https://www.R-project.org/.

Richter, H. 1997. "Water Relations in the Field: Some Comments on the Measurement of Selected Parameters." *Journal of Experimental Botany* 48: 1–7. https://doi.org/10.1093/jxb/48.1.1.

Rodriguez-Dominguez, C. M., A. Forner, S. Martorell, et al. 2022. "Leaf Water Potential Measurements Using the Pressure Chamber: Synthetic Testing of Assumptions Towards Best Practices for Precision and Accuracy." *Plant, Cell & Environment* 45: 2037–2061. https://doi.org/10.1111/pce.14330.

Sánchez-Costa, E., R. Poyatos, and S. Sabaté. 2015. "Contrasting Growth and Water Use Strategies in Four Co-Occurring Mediterranean Tree Species Revealed by Concurrent Measurements of Sap Flow and Stem Diameter Variations." *Agricultural and Forest Meteorology* 207: 24–37. https://doi.org/10.1016/j.agrformet.2015.03.012.

Scholander, P. F., E. D. Bradstreet, E. A. Hemmingsen, and H. T. Hammel. 1965. "Sap Pressure in Vascular Plant: Negative Hydrostatic Pressure Can Be Measured in Plants." *Science* 148: 339–346. https://doi.org/10.1126/science.148.3668.339.

Scholz, F. G., S. J. Bucci, G. Goldstein, F. C. Meinzer, A. C. Franco, and F. Miralles-Wilhelm. 2007. "Biophysical Properties and Functional Significance of Stem Water Storage Tissues in Neotropical Savanna Trees." *Plant, Cell & Environment* 30: 236–248. https://doi.org/10.1111/j.1365-3040.2006.01623.x.

Scholz, F. G., N. G. Phillips, S. J. Bucci, F. C. Meinzer, and G. Goldstein. 2011. "Hydraulic Capacitance: Biophysics and Functional Significance of Internal Water Sources in Relation to Tree Size." In *Size- and Age-Related Changes in Tree Structure and Function*, edited by F. C. Meinzer, B. Lachenbruch, and T. E. Dawson. Dordrecht, Netherlands: Springer Science & Business Media.

Schuldt, B., A. Buras, M. Arend, et al. 2020. "A First Assessment of the Impact of the Extreme 2018 Summer Drought on Central European Forests." *Basic and Applied Ecology* 45: 86–103. https://doi.org/10.1016/j.baae.2020.04.003.

Sevanto, S., E. Nikinmaa, A. Rikkonen, et al. 2008. "Linking Xylem Diameter Variation With Sap Flow Measurements." *Plant and Soil* 305: 77–90. https://doi.org/10.1007/s11104-008-9566-8.

Steppe, K. 2018. "The Potential of the Tree Water Potential." *Tree Physiology* 38: 937–940. https://doi.org/10.1093/treephys/tpy064.

Stöhr, A., and R. Lösch. 2004. "Xylem Sap Flow and Drought Stress of *Fraxinus excelsior* Sapling." *Tree Physiology* 24: 169–180. https://doi.org/10.1093/treephys/24.2.169.

Szatniewska, J., I. Zavadilova, O. Nezval, et al. 2022. "Species-Specific Growth and Transpiration Response to Changing Environmental Conditions in Floodplain Forest." *Forest Ecology and Management* 516: 120248. https://doi.org/10.1016/j.foreco.2022.120248.

Torres-Ruiz, J. M., H. Cochard, S. Delzon, et al. 2024. "Plant Hydraulics at the Heart of Plant, Crops and Ecosystem Functions in the Face of Climate Change." *New Phytologist* 241: 984–999. https://doi.org/10.1111/nph.19463.

Villalobos, F. J., L. Testi, O. García-Tejera, Á. López-Bernal, I. Tejado, and B. M. Vinagre. 2024. "Measuring the Diurnal Variation of Root Conductance in Olive Trees Using Microtensiometers and Sap Flow Sensors." *Plant and Soil*. https://doi.org/10.1007/s11104-024-06873-7.

Wankmüller, F. J. P., L. Delval, P. Lehmann, et al. 2024. "Global Influence of Soil Texture on Ecosystem Water Limitation." *Nature* 635: 631–638. https://doi.org/10.1038/s41586-024-08089-2.

Werner, C., U. Wallrabe, A. Christen, L. Comella, C. Dormann, and A. Göritz. 2024. "ECOSENSE-Multi-Scale Quantification and Modelling of Spatio-Temporal Dynamics of Ecosystem Processes by Smart Autonomous Sensor Networks." *Research Ideas & Outcomes* 10: e129357. https://doi.org/10.3897/rio.10.e129357.

Wullschleger, S. D., F. C. Meinzer, and R. A. Vertessy. 1998. "A Review of Whole-Plant Water Use Studies in Trees." *Tree Physiology* 18: 499–512. https://doi.org/10.1093/treephys/18.8-9.499.

Ziegler, Y., R. Grote, F. Alongi, T. Knüver, and N. K. Ruehr. 2024. "Capturing Drought Stress Signals: The Potential of Dendrometers for Monitoring Tree Water Status." *Tree Physiology* 44: tpae140. https://doi.org/10.1093/treephys/tpae140.

Zweifel, R., M. Haeni, N. Buchmann, and W. Eugster. 2016. "Are Trees Able to Grow in Periods of Stem Shrinkage?" *New Phytologist* 211: 839–849. https://doi.org/10.1111/nph.13995.

Zweifel, R., H. Item, and R. Häsler. 2001. "Link Between Diurnal Stem Radius Changes and Tree Water Relations." *Tree Physiology* 21: 869–877. https://doi.org/10.1093/treephys/21.12-13.869.

Supporting Information

Additional supporting information can be found online in the Supporting Information section.